

Flow-induced whisker orientation and viscosity for molten composite systems in a uniaxial elongational flow field

Masatoshi Kobayashi, Tatuhiro Takahashi, Junichi Takimoto and Kiyohito Koyama*

Department of Materials Science and Engineering, Yamagata University, 4-3-16 Jonan, Yonezawa, Yamagata 992, Japan

(Received 20 October 1994; revised 24 April 1995)

The elongational viscosity of polystyrene–potassium titanate whisker composite melt was estimated by using a Meissner-type uniaxial elongational rheometer. The time dependence of flow-induced whisker orientation in a uniaxial elongational flow field was analysed in terms of the average polar angle with respect to the flow direction by wide-angle X-ray diffraction, in order to study the influence of whisker orientation on the elongational viscosity of composite melts. The whiskers prevented the strain-hardening phenomenon in elongational flow for polystyrene. The elongational viscosity was almost independent of the orientational change of the whiskers. The orientation of the whiskers was dependent on strain only. To understand this phenomenon, whisker orientation was discussed in comparison with Jeffery theory. The tendencies of the average polar angle were similar to the tendency of Jeffery theory in a uniaxial elongational flow field.

(Keywords: whisker; elongational viscosity; flow-induced orientation)

INTRODUCTION

In the past ten years there has been increasing interest in preparing polymer–inorganic composites in the plastics industry. These composites have important merits to improve stiffness, strength and heat distortion temperature in comparison with unfilled polymers. When polymers are reinforced with geometrically anisotropic fillers, e.g. fibre-shaped fillers or plate-shaped fillers, the mechanical properties of the composites are affected by the orientation of the fillers. Therefore, it is of interest to consider the relation between moulding conditions and filler orientation induced by flow from the standpoint of polymer processing.

There have been diverse reports about flow-induced filler orientation^{1–6}. Some papers have reported that the degree of flow-induced filler orientation increases with the increase of shear rate or flow rate^{1–3}. In contrast, other papers have reported that the degree of orientation decreases with increasing shear rate or flow rate⁴, or has a maximum value at some critical shear rate⁵. In spite of similar experimental treatments, different results have been reported on the influence of capillary length at the same shear rate: the degree of orientation decreases² or increases³ with increasing capillary length, or has a maximum value at a certain length^{5,6}. Such contradictory results are surely attributed to the complicated flow in injection or extrusion moulding, for instance, non-isothermal flow, flow with both shear and elongational components, etc. To resolve such ambiguous points,

measurements must be carried out for flow-induced filler orientation in a simple and isothermal flow field. Nevertheless, there has been no report on the experimental study of filler orientation in a simple uniaxial elongational flow field. This investigation has the possibility to provide variable information for polymer processing, since uniaxial elongational flow dominates in the entrance part of a capillary for injection or extrusion moulding.

Many computer simulations^{7–10} have predicted fibre orientation in mouldings of fibre-reinforced polymers using equations based on Jeffery theory¹¹. However, it is not clear whether the theory agrees quantitatively with flow-induced fibre orientation. The main reason is that the parameters reflecting the orientation have not been clarified experimentally. To clarify the parameters, the comparison must be made in a simple and isothermal flow field instead of the complex flow field in moulding machines.

Understanding the influence of filler orientational change on the viscosity of composite melts is important. Laun¹² reported that the change of fibre orientation during shear flow gives rise to a pronounced overshoot of shear stress and of normal stress by comparing polystyrene–acrylonitrile filled with glass fibres and that filled with glass beads. Judging from their result¹², it may be expected that the change of fibre orientation became more remarkable when the overshoot was observed. The analysis of this phenomenon, however, has never been constructed because of the difficulty in estimating the effect of orientational change on rheological properties, as the rheological behaviour of

* To whom correspondence should be addressed



Figure 1 SEM photomicrograph of potassium titanate whiskers

Table 1 Sample code and fraction of whiskers for composites

Sample code	Whisker content	
	(vol%)	(wt%)
PSTI-5	5	14
PSTI-10	10	26

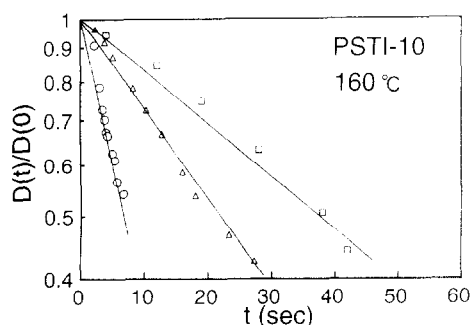


Figure 2 Time variation of the common logarithm of rod-shaped sample diameter for PSTI-10 during elongational flow: (○) 0.27 s^{-1} ; (△) 0.070 s^{-1} ; (□) 0.038 s^{-1}

filler-reinforced polymers is sensitive to filler size, surface condition, filler content and so on. Even so, both the rheological and the fibre orientation data must be taken into consideration to discuss the effect of the orientational change of fibres on the viscosity of a composite material.

In this paper, we have examined the effects of potassium titanate whiskers on the elongational viscosity of polystyrene (PS) melt using a Meissner-type uniaxial elongational rheometer¹³. We have also measured the time dependence of whisker orientation during elongation by wide-angle X-ray diffraction in order to discuss the influence of orientational change on the elongational viscosity. Furthermore, efforts have been made to clarify the parameter reflecting flow-induced whisker orientation through a comparison between experimental data and the theoretical values calculated according to Jeffery theory.

EXPERIMENT

Materials

The polymer used in this study was a commercial polystyrene (Idemitsu Styrol HH-30; $M_w = 2.6 \times 10^5$, $M_w/M_n = 2.8$) supplied by Idemitsu Petrochemical Co. The fibre-shaped filler used in this study was a commercial potassium titanate whisker (TISMO-D; length = $10\text{--}20 \mu\text{m}$, diameter = $0.2\text{--}0.5 \mu\text{m}$, relative density = $3.3\text{--}3.4$) supplied by Ootuka Chemical Co. Figure 1 shows a scanning electron micrograph of the potassium titanate whiskers. Before mixing, the whiskers were annealed at 1000°C for 3 h to obtain a well crystallized sample¹⁴. The polystyrene and the whiskers were mixed by using a twin-screw mixer and were subsequently pelletized. Rod-shaped composite samples were prepared by using a single-screw extruder. The rod-shaped samples of neat polystyrene were also prepared in the same way as above. These samples had uniform diameter of about 3 mm, and length of about 40 cm. The contents of the whiskers are 5 and 10 vol%. These are designated as PSTI-5 and PSTI-10 respectively. The sample code and fraction of whiskers are shown in Table 1. For these whisker contents, the rotational motion of the whiskers is restricted by the interaction among them.¹⁵

Elongational viscosity

The uniaxial elongational viscosity of the composite melts was measured by using a Meissner-type elongational rheometer. The apparatus was the same as those reported in our previous study¹⁶. The distance between the two clamps was 18 cm. A rod-shaped sample was held in a bath filled with silicone oil KF50-100cs (Shinetsu Chemical Co.) and was melted at 160°C for 10 min. Then the sample was elongated at a constant strain rate. By monitoring a rod-shaped sample during elongation by CCD camera (Photron Co. Ltd, CCD video camera module), the time variation of the diameter of the sample was recorded with a videotape recorder. The elongational strain is defined by the following equation:

$$\epsilon = \ln(l/l_0) \quad (1)$$

Here l_0 and l are the initial and the instantaneous length of the rod-shaped sample, respectively; ϵ is called the Hencky strain.

According to previous reports¹⁶⁻¹⁹ on elongational viscosity measurements, unfilled polymers can be deformed uniformly, but such uniform deformation must also be confirmed for filled polymer systems. In doing so, an accurate strain rate was calculated by using the following equation:

$$D(t)/D(0) = \exp(-\dot{\epsilon}t/2) \quad (2)$$

Here $D(t)$ is the time variation of the diameter of a rod-shaped sample, and $\dot{\epsilon}$ is the elongational strain rate.

Figure 2 shows the time variation of the common logarithm of the rod-shaped sample diameter for PSTI-10 during elongational flow. Since the points lie on a straight line, uniformity of elongational deformation under constant strain rate was assured for the molten composite. In this way, it was confirmed that uniform uniaxial elongational deformation was attained for composite melts as well as for homogeneous polymer melts.

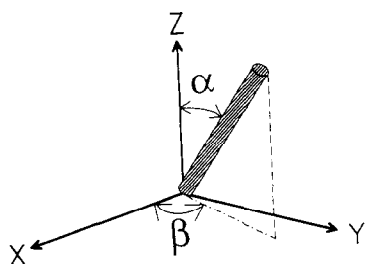


Figure 3 Coordinate system X , Y , Z used in determination of the fibre-shaped filler orientation. The Z axis is the direction of elongational flow; α is the angle between the flow direction and main axis of the fibre

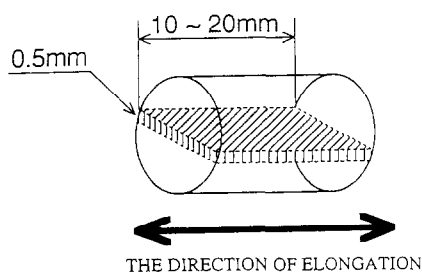


Figure 4 Sketch of the cut and quenched sample

Flow-induced whisker orientation

When the fillers are not spherical but flat or fibre shaped, those anisotropic fillers are oriented in a direction so that the flow resistance is the smallest. Therefore, the major axis of anisotropic fillers tends to align parallel to the flow direction. Such a flow-induced anisotropic filler orientation is affected not only by hydrodynamic action but also by interaction among the filler particles. However, it is difficult to evaluate the latter interaction. For a suspension of fibrous fillers with length L and diameter D , the interaction is discussed in relation to the number of filler particles per unit volume, n . Three stages of concentration¹⁵ are proposed: dilute concentration, in which $n \ll 1/L^3$; semi-concentrated concentration, $1/L^3 < n < 1/DL^2$; and high concentration, $n \gg 1/DL^2$. In our experiment, the concentration of whiskers in the composites obviously is the highest in the third stage.

Einstein²⁰ formulated the rotary motion theory of spherical-shaped fillers in a Newtonian fluid. Jeffery¹¹ expanded Einstein's theory and studied the theory of flow-induced anisotropic filler orientation in a Newtonian fluid. Takserman-Krozer and Ziabicki²¹ applied the Jeffery theory to an elongational flow field. The rotary motion equation and its solution are as follows:

$$\frac{d\beta}{dt} = 0 \quad \frac{d\alpha}{dt} = -\frac{3}{4}\dot{\epsilon}R \sin(2\alpha) \quad (3)$$

where

$$R = \frac{r_p^2 - 1}{r_p^2 + 1}$$

and

$$\tan \alpha = \exp\left(-\frac{3}{2}\dot{\epsilon}Rt\right) \tan \alpha_0 \quad (4)$$

Here R is the shape factor determined by the aspect ratio, r_p the aspect ratio, $\dot{\epsilon}$ the elongational strain rate, α_0 the initial orientation angle, and α and β the orientation

angles in the coordinate system used (Figure 3). The average of r_p for the whiskers is 43. In this equation, the interaction among fillers is not considered.

Dinh and Armstrong²² proposed theoretically that flow-induced filler orientation depends only on strain. In their equations, the interaction among fillers is considered to some extent. The equation in an elongational flow field is as follows:

$$\tan \alpha = \exp\left(-\frac{3}{2}\epsilon\right) \tan \alpha_0 \quad \beta = \beta_0 \quad (5)$$

It is recognized that flow-induced orientation of anisotropic fillers in an elongational flow field does not have periodic rotary motion and indicates monotonic increase in the flow direction from not only equation (5) but also equation (4). Equations (4) and (5) are equal, because R is almost unity when the aspect ratio is large enough. This fact is explained by assuming that the interaction among fillers increases with the increase of the aspect ratio. Equation (4) was used for theoretical prediction in this paper.

The orientation of fibre-shaped fillers is measured by using optical microscopy, scanning electron microscopy, light scattering, soft X-ray diffraction, or wide-angle X-ray diffraction, etc. Menendez *et al.*⁶ measured the orientation of Kevlar (poly(*p*-phenylene terephthalamide)) in composites by using wide-angle X-ray diffraction. Takeda and Seino^{23,24} measured the orientation of potassium titanate whiskers in composites by using wide-angle X-ray diffraction. We use the same composite samples as Takeda and Seino. Therefore, the measurement of flow-induced whisker orientation in an elongational field was carried out by a wide-angle X-ray diffractometer RAD-rA (Rigaku Denki Co. Ltd) with Ni-filtered $\text{Cu K}\alpha$ radiation. X-ray diffraction was measured by using the transmission method. The molten samples during elongation were cut with both ends fixed to prevent shrinkage of the sample, then quenched in ice-water as quickly as possible. Figure 4 shows a sketch of the cut and quenched sample. We filed the middle part of the sample subsequently. The thickness of the filed sample is about 0.5 mm. We did not monitor the diameter change of the sample during elongation because the CCD camera obstructed the quick-quenching procedure. Thus, the strain rate for the whisker orientation measurement was assumed to be the same as the accurate strain rate for the same kind of sample and the same conditions. In meridional and equatorial scans, the filed sample was set so that the direction of the incident X-ray beam and the flow direction of the sample are perpendicular. A typical equatorial scan for PS and meridional and equatorial scans for PSTI-10 after elongation are shown in Figure 5. The whisker orientation can be characterized by the 020 reflection, because the whiskers grow in the direction of the b -axis. The amorphous halo of PS did not disturb the 020 reflection. In the polar angle intensity scans, the sample was set so that the direction of the incident X-ray beam and the flow direction of the sample are at an angle of θ degrees. Figure 6 shows the polar angle intensity distribution of the 020 reflection for PSTI-10. The angle on the meridian is 0° . It is noticed that the whiskers before elongation take almost a random orientation and those after elongation are oriented predominantly in the elongational direction. The degree of whisker orientation

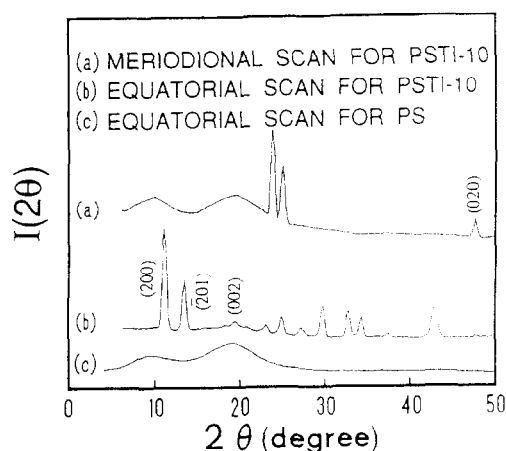


Figure 5 Typical equatorial scan for PS (c) and equatorial (b) and meridional (a) scans for PSTI-10

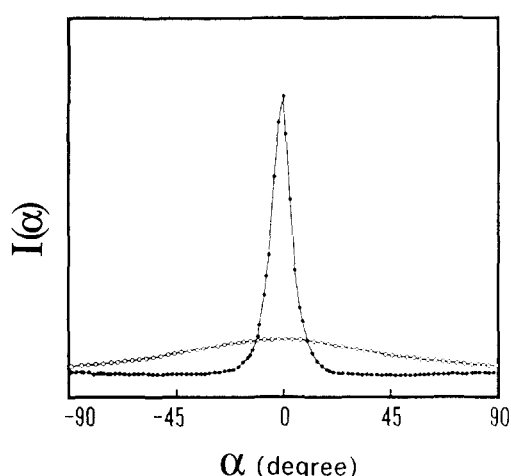


Figure 6 Polar angle intensity distribution of the 020 reflection for PSTI-10: (○) before elongation; (●) elongated at 0.0042 s^{-1} for 417 s

was estimated in terms of the average polar angle $\langle\alpha\rangle$ from the data of the intensity distribution, which is defined by:

$$\langle\alpha\rangle = \frac{\int_0^{\pi/2} \alpha I(\alpha) \sin \alpha d\alpha}{\int_0^{\pi/2} I(\alpha) \sin \alpha d\alpha} \quad (6)$$

where $\langle\alpha\rangle$ is the average polar angle and $I(\alpha)$ the intensity at α .

Equation (4) shows the orientational behaviour of a single fibre without considering the orientation distribution. The respective whiskers before elongation take various orientation angles. From the theory, a fibre-shaped filler rotates with orientation angular velocity changing step by step. The angular velocity is largest when the fibre orientation angle is $\pm 45^\circ$ to the flow direction. However, if Jeffery theory can be applied to the flow-induced orientation of fibre-shaped fillers in an elongational field, the theoretical behaviour of a single whisker and the experimental average behaviour of many whiskers should show a similar tendency. Then the theoretical behaviour of α for a single whisker was compared with that of $\langle\alpha\rangle$. The theoretical values α were

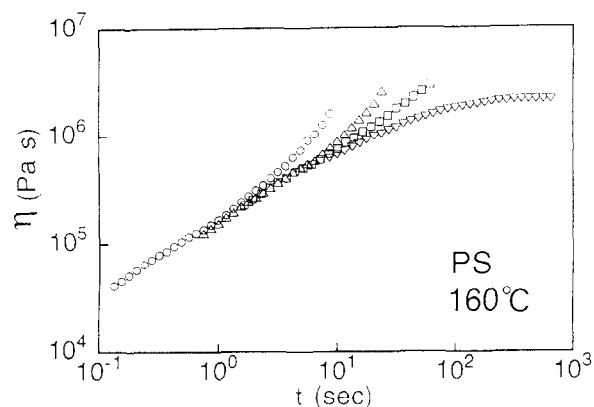


Figure 7 Transient elongational viscosity curves for PS: (○) 0.38 s^{-1} ; (Δ) 0.11 s^{-1} ; (□) 0.039 s^{-1} ; (▽) 0.0030 s^{-1}

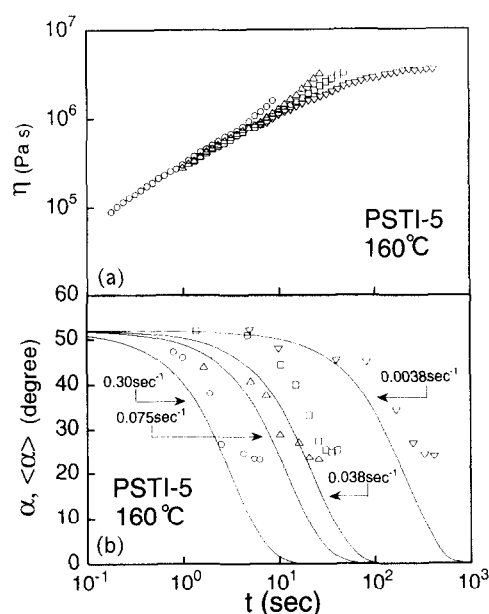


Figure 8 (a) Transient elongational viscosity curves and (b) comparison of the average polar angle $\langle\alpha\rangle$ for PSTI-5 and Jeffery theory α for a single whisker: (○) 0.30 s^{-1} ; (Δ) 0.075 s^{-1} ; (□) 0.038 s^{-1} ; (▽) 0.0038 s^{-1} . The solid line is Jeffery theory calculated from equation (4)

calculated by using α_0 equal to $\langle\alpha\rangle$ for the sample before elongation, respectively.

RESULTS AND DISCUSSION

Influence of whisker orientation on elongational viscosity

Figure 7 shows the transient elongational viscosity curves for neat PS. The elongational viscosity at low strain rate gradually increases with time at first and reaches a steady state in the long-time region (the linear viscoelastic region). The viscosity at high strain rate also gradually increases with time at first, but after a critical time, it increases more rapidly at large strain (the non-linear viscoelastic region). The critical time decreases with increasing strain rate. Figures 8a and 9a show transient elongational viscosity curves for PSTI-5 and PSTI-10. The behaviour of the elongational viscosity for PSTI-5 is almost the same as that for neat PS at both low and high strain rates. The slope of the curves in the

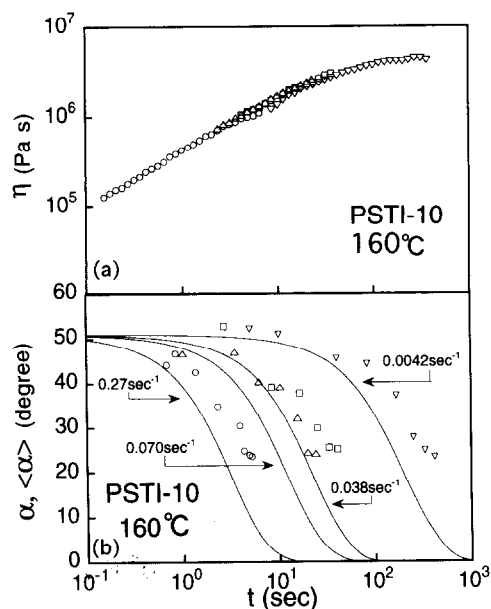


Figure 9 (a) Transient elongational viscosity curves and (b) comparison of the average polar angle $\langle\alpha\rangle$ for PSTI-10 and Jeffery theory α for a single whisker: (○) 0.27sec^{-1} ; (△) 0.070sec^{-1} ; (□) 0.038sec^{-1} ; (▽) 0.0042sec^{-1} . The solid line is Jeffery theory calculated from equation (4)

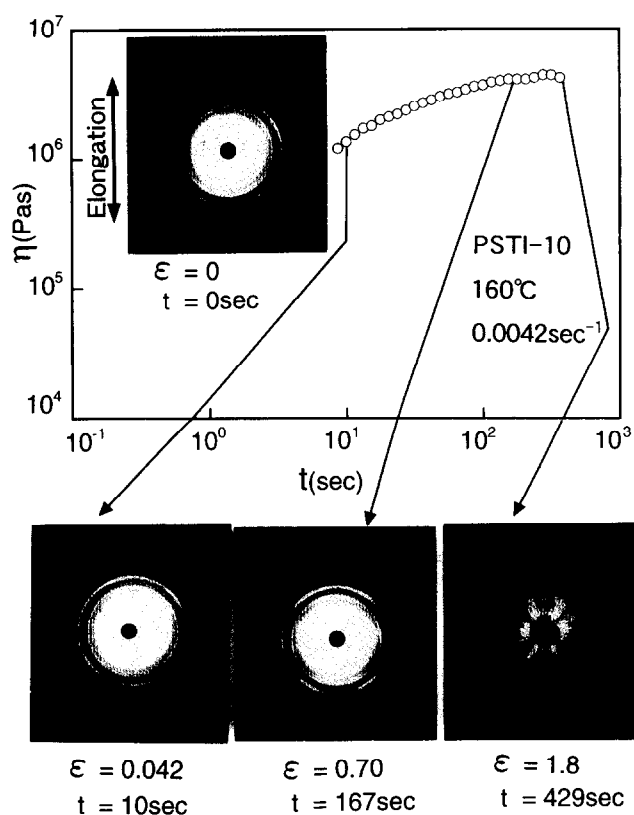


Figure 10 Transient elongational viscosity curves and corresponding X-ray diffraction patterns for PSTI-10

non-linear viscoelastic region slightly decreases. For the behaviour of the elongational viscosity for PSTI-10, no rapid increase of the viscosity curves is observed not only at lower strain rate but also at higher strain rate. Through these experimental results, it turns out that the whiskers suppress the non-linearity in the elongational viscosity for PS. That is, the elongational viscosity in the

linear viscoelastic region increases with increasing filler content while the non-linear viscoelastic phenomenon is prevented with increasing filler content. Such phenomena were also confirmed in the elongational viscosity for polymer melt reinforced with spherical-shaped fillers (for example, glass bead-reinforced high-density polyethylene melts²⁵ and carbon black-reinforced polystyrene melts²⁶). This means that the results shown in Figures 8a and 9a are typical tendencies for composite systems.

Figure 10 shows the transient elongational viscosity curve for PSTI-10 obtained at 0.0042sec^{-1} and corresponding X-ray diffraction patterns. The whiskers before elongational flow are almost randomly oriented. The azimuthal breadth in the X-ray diffraction pattern is decreased with strain or time, indicating the development of flow-induced whisker orientation in the elongational direction. The whisker orientation increases remarkably from elongational time = 167 to 429 s, while the elongational viscosity is almost constant in this range. Figures 8b and 9b show the comparison between the theoretical value α and $\langle\alpha\rangle$ for PSTI-5 and PSTI-10 respectively. The whisker orientational behaviour for both PSTI-5 and PSTI-10 shows a similar tendency. The orientation is induced at all elongational strain rates in the flow direction by elongational flow, and thus the orientational degree increases with increasing time. The orientational degree increases with increasing elongational strain rate at short timescale. Though the behaviours of the whisker orientation for PSTI-5 and PSTI-10 resemble each other, the corresponding behaviour of the elongational viscosity for these is different. Such behaviour is quite different from Laun's result¹² that the change of orientation causes a significant effect on viscoelastic properties under shear flow. If this is the case, change of the viscosity curves must be recognized when the change of the whisker orientation is remarkable. The influence should be more remarkable by increasing the filler content. However, the results indicate no effect of orientational change of the whisker on the elongational viscosity in the given range of strain rate. To obtain conclusive evidence for the influence of orientational change on the elongational viscosity, similar experiments to those shown in Figures 8 and 9 must be carried out under more greatly varying conditions of fibre concentration, fibre length, aspect ratio, etc. If fibre size cannot be ignored compared with the diameter of rod-shaped samples, the influence of orientation change in an elongational flow field may appear.

Behaviour of whisker orientation and Jeffery theory

Figures 8b and 9b show the comparison of Jeffery theory and whisker orientational degree for PSTI-5 and PSTI-10. Although the absolute value of $\langle\alpha\rangle$ cannot be compared with that of the theoretical value α , the decreasing tendency of $\langle\alpha\rangle$ for both PSTI-5 and PSTI-10 at all elongational strain rates is similar to that of Jeffery's theoretical curve proposed by Takserman-Krozer and Ziabicki. Figures 11 and 12 show α and $\langle\alpha\rangle$ with Hencky strain. In this case, α can be determined by the strain given to the materials independent of the elongational strain rate. The value of $\langle\alpha\rangle$ decreases with increasing strain monotonically and tends to level off. The behaviour for PSTI-5 almost agrees with that for PSTI-10. The $\langle\alpha\rangle$ value indicates a steady state above about Hencky strain = 1.2 in both PSTI-5 and PSTI-10.

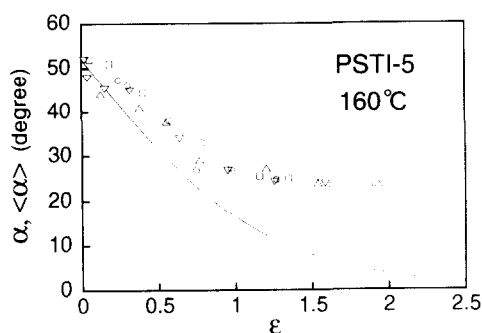


Figure 11 The average polar angle $\langle \alpha \rangle$ for PSTI-5 and Jeffery theory α for a single whisker with Hencky strain: (○) 0.30 s⁻¹; (△) 0.075 s⁻¹; (□) 0.038 s⁻¹; (▽) 0.0038 s⁻¹. The solid line is Jeffery theory calculated from equation (4)

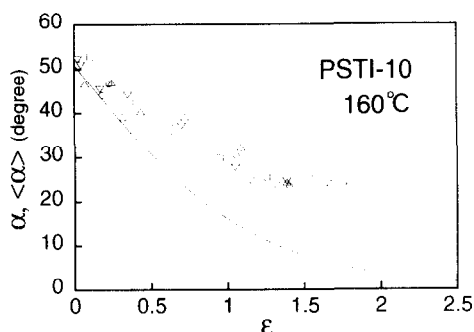


Figure 12 The average polar angle $\langle \alpha \rangle$ for PSTI-10 and Jeffery theory α for a single whisker with Hencky strain: (○) 0.27 s⁻¹; (△) 0.070 s⁻¹; (□) 0.038 s⁻¹; (▽) 0.0042 s⁻¹. The solid line is Jeffery theory calculated from equation (4)

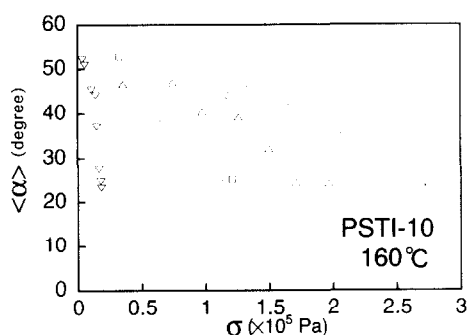


Figure 13 The average polar angle $\langle \alpha \rangle$ for PSTI-10 with stress given to the materials: (○) 0.27 s⁻¹; (△) 0.070 s⁻¹; (□) 0.038 s⁻¹; (▽) 0.0042 s⁻¹

In this experiment, equation (5) almost agrees with equation (4), because R calculated using the aspect ratio of the whiskers, $r_p = 43$, is approximately unity. Therefore, the tendencies of $\langle \alpha \rangle$ are also similar to the other theoretical curve proposed by Dinh and Armstrong. These results imply that flow-induced whisker orientation under elongational flow can be predicted approximately by the theories by Jeffery and Dinh *et al.*

Parameter of flow-induced whisker orientation

It should be noted that the orientation of a molecular chain of a polymer during flow is expressed by the stress-optical law²⁷⁻³⁰ $\Delta n = C\sigma$. The stress-optical coefficient C is a constant for respective polymers. Wales²⁷ measured the birefringence in steady shear flow and

showed the validity of the stress-optical law. Gortemaker *et al.*^{28,29} measured the birefringence and stress of polyethylene and polystyrene under transient shear flow. Koyama and Ishizuka³⁰ measured the birefringence and stress of low-density polyethylene under transient elongational flow. These reports pointed out that the degree of molecular orientation during flow is determined not by the strain rate but by the stress given to the materials. Accordingly it must be confirmed whether flow-induced whisker orientation is determined by the stress given to the materials. Figure 13 shows $\langle \alpha \rangle$ for PSTI-10 with increasing stress given to the materials at various strain rates. The $\langle \alpha \rangle$ value decreases with increase of stress at all strain rates. It is clear that the decreasing behaviour of $\langle \alpha \rangle$ exhibits different modes at the indicated elongational strain rates. This means that the orientational behaviour of the molecular chain of a polymer is different from that of fillers. The $\langle \alpha \rangle$ values are determined only by the strain given to the materials independent of the elongational strain rate.

CONCLUSION

Measurements were carried out for flow-induced whisker orientation and the viscosity of polystyrene-potassium titanate whisker composites in a uniaxial elongational flow field. Whiskers in composite melts prevent the strain-hardening phenomenon under uniaxial elongational flow. The effect of whisker orientational change on the elongational viscosity was not recognized. The decreasing tendencies of the average polar angle $\langle \alpha \rangle$ for PSTI-5 almost agree with that for PSTI-10. The $\langle \alpha \rangle$ value was found to be determined only by the strain given to the materials. The $\langle \alpha \rangle$ value reached steady state at Hencky strain >1.2 in both PSTI-5 and PSTI-10. The decreasing tendencies of $\langle \alpha \rangle$ were similar to that of the Jeffery theory.

ACKNOWLEDGEMENTS

The authors thank Mr H. Murakami for help with some of the experiments and express appreciation to Mr M. Shinohara of Idemitsu Petrochemical Co. for providing the samples. The authors also gratefully acknowledge Dr H. Takeda for valuable discussions and comments on many points.

REFERENCES

- 1 Knutsson, B. A., White, J. M. and Abbas, K. B. *J. Appl. Polym. Sci.* 1981, **26**, 2347
- 2 Crowson, R. J., Folkes, M. J. and Bright, P. F. *Polym. Eng. Sci.* 1980, **20**, 925
- 3 Vaxman, A., Narkis, M., Siegmann, A. and Kenig, S. *J. Mater. Sci. Lett.* 1988, **7**, 25
- 4 Bright, P. F., Crowson, R. J. and Folkes, M. J. *J. Mater. Sci.* 1978, **13**, 2497
- 5 Wu, S. *Polym. Eng. Sci.* 1979, **19**, 638
- 6 Menendez, H. and White, J. L. *Polym. Eng. Sci.* 1984, **24**, 1051
- 7 Folgar, F. and Tucker, C. L. *J. Reinf. Plast. Compos.* 1982, **3**, 98
- 8 Goldsmith, H. L. and Mason, S. G. 'Rheology' (Ed. F. R. Eirich), Vol. 4, Academic Press, New York, 1964
- 9 Givler, R. C., Crochet, M. J. and Pipes, R. B. *J. Compos. Mater.* 1983, **17**, 330
- 10 Vincent, M. and Agassant, J. F. *Polym. Compos.* 1986, **7**, 76
- 11 Jeffery, G. B. *Proc. R. Soc. (A)* 1922, **102**, 161
- 12 Laun, H. L. *Colloid Polym. Sci.* 1984, **262**, 257
- 13 Meissner, J. *Rheol. Acta* 1969, **8**, 78

- 14 Shimizu, T., Hashimoto, K. and Yanagida, H. *Yogyo-Kyokai-Shi. Japan* 1977, **85**, 41
- 15 Doi, M. and Edwards, S. F. in 'The Rheology of Polymer Dynamics', Oxford Science Publications, 1986
- 16 Ishizuka, O. and Koyama, K. *Polymer* 1980, **21**, 164
- 17 Koyama, K. and Ishizuka, O. *J. Soc. Rheol. Japan* 1985, **13**, 93
- 18 Yoshikawa, K., Toneaki, N., Moteki, Y., Takahashi, M. and Masuda, T. *J. Soc. Rheol. Japan* 1990, **18**, 80
- 19 Shinohara, M. *J. Soc. Rheol. Japan* 1991, **19**, 8118
- 20 Einstein, A. *Ann. Physik.* 1906, **19**, 289
- 21 Takserman-Krozer, R. and Ziabicki, A. *J. Polym. Sci.* 1963, **1**, 491
- 22 Dinh, S. M. and Armstrong, R. C. *J. Rheol.* 1984, **28**, 207
- 23 Takeda, H. and Seino, Y. *Seikeikakou* 1989, **1**, 88
- 24 Takeda, H. and Seino, Y. *Seikeikakou* 1989, **1**, 197
- 25 Kobayashi, M., Minagawa, K., Takeda, H., Iwakura, K. and Koyama, K. *Proc. Polym. Process. Soc.-Toyko '93*, 1993, p. 167
- 26 Lobe, V. M. and White, J. L. *Polym. Eng. Sci.* 1979, **19**, 617
- 27 Wales, J. L. S. 'The Application of Flow Birefringence to Rheological Studies of Polymer Melts', Delft University, Rotterdam, 1976
- 28 Gortemaker, F. H., Hansen, M. G., de Cindio, B. and Janeschitz-Kriegl, H. *Rheol. Acta* 1976, **15**, 242
- 29 Gortemaker, F. H., Hansen, M. G., de Cindio, B., Laun, H. M. and Janeschitz-Kriegl, H. *Rheol. Acta* 1976, **15**, 256
- 30 Koyama, K. and Ishizuka, O. *J. Polym. Sci., Polym. Phys. Edn.* 1989, **27**, 297.